



HAL
open science

Imaging of extracellular cathepsin S activity by a selective near infrared fluorescence substrate-based probe

Mylène Wartenberg, Ahlame Saidi, Mathieu Galibert, Alix Joulin-Giet, Julien Burlaud-Gaillard, Fabien Lecaille, Christopher Scott, Vincent Aucagne, A.F. Delmas, Gilles Lalmanach

► **To cite this version:**

Mylène Wartenberg, Ahlame Saidi, Mathieu Galibert, Alix Joulin-Giet, Julien Burlaud-Gaillard, et al.. Imaging of extracellular cathepsin S activity by a selective near infrared fluorescence substrate-based probe. *Biochimie*, 2019, 166, pp.84-93. 10.1016/j.biochi.2019.03.013 . hal-02088627

HAL Id: hal-02088627

<https://hal.science/hal-02088627>

Submitted on 20 Jul 2022

HAL is a multi-disciplinary open access archive for the deposit and dissemination of scientific research documents, whether they are published or not. The documents may come from teaching and research institutions in France or abroad, or from public or private research centers.

L'archive ouverte pluridisciplinaire **HAL**, est destinée au dépôt et à la diffusion de documents scientifiques de niveau recherche, publiés ou non, émanant des établissements d'enseignement et de recherche français ou étrangers, des laboratoires publics ou privés.



Distributed under a Creative Commons Attribution - NonCommercial 4.0 International License

Imaging of extracellular cathepsin S activity by a selective near infrared fluorescence substrate-based probe

Mylène Wartenberg ^{a, b, 1}, Ahlame Saidi ^{a, b, 1}, Mathieu Galibert ^{c, 2}, Alix Joulin-Giet ^{a, b, 3}, Julien Burlaud-Gaillard ^{a, d}, Fabien Lecaille ^{a, b}, Christopher J. Scott ^e, Vincent Aucagne ^c, Agnès F. Delmas ^c, & Gilles Lalmanach ^{a, b, 4}

^a Université de Tours, Tours, France

^b INSERM, UMR 1100, Research Center for Respiratory Diseases (CEPR), Team: "Proteolytic Mechanisms in Inflammation", Tours, France

^c CNRS UPR 4301, Center for Molecular Biophysics (CBM), Team: "Molecular, Structural and Chemical Biology", Orléans, France

^d Plateforme IBiSA de Microscopie Electronique, Université de Tours, Tours, France

^e Centre for Cancer Research and Cell Biology, School of Medicine, Dentistry and Biomedical Sciences, Queen's University Belfast, Belfast, Northern Ireland, UK

Footnotes:

¹ MW & AS: Equal contribution to the work

² Current address: GENEPEP, Saint-Jean-de-Védas, France

³ Current address: Innate Pharma SA, Marseille, France

⁴ Corresponding author : Prof Gilles Lalmanach, INSERM UMR1100, Centre d'Etude des Pathologies Respiratoires (CEPR), Equipe « Mécanismes protéolytiques dans l'inflammation », Université de Tours, Faculté de Médecine, 10 Boulevard Tonnellé, 37032 Tours cedex, France. Tel: (+33) 2 47 36 61 51, Mail: gilles.lalmanach@univ-tours.fr

Abstract

We designed a near-infrared fluorescent substrate-based probe (SBP), termed MG101, for monitoring extracellular cathepsin S (CatS) activity. We conceived a fused peptide hairpin loop-structure, combining a CatS recognition domain, an electrostatic zipper (with complementary charges of a polyanionic (D-Glu)₅ segment and a polycationic (D-Arg)₅ motif, as well as a N- and C- terminal Förster resonance energy transfer pair (donor: AlexaFluor680; quencher: BHQ3) to facilitate activity-dependent imaging. MG101 showed excellent stability since no fluorescence release corresponding to a self-dequenching was observed in the presence of either 2 M NaCl or after incubation at a broad range of pH (2.2-8.2). Cathepsins B, D, G, H, and K, neutrophil elastase and proteinase 3 did not cleave MG101, while CatS, and to a lesser extent CatL, hydrolysed MG101 at pH5.5. However MG101 was fully selective for CatS at pH 7.4 ($k_{cat}/K_m=140,000 \text{ M}^{-1}\cdot\text{s}^{-1}$) and sensitive to low concentration of CatS (<1 nM). The selectivity of MG101 was successfully endorsed *ex vivo*, as it was hydrolysed in cell lysates derived from wild-type but not knockout CatS murine spleen. Furthermore, application of the SBP probe with confocal microscopy confirmed the secretion of active CatS from THP-1 macrophages, which could be abrogated by pharmacological CatS inhibitors. Taken together, present data highlight MG101 as a novel near-infrared fluorescent SBP for the visualization of extracellular active CatS from macrophages and other cell types.

Keywords: Cysteine cathepsin; Förster resonance energy transfer (FRET); Macrophage; Near-infrared fluorescence (NIRF); Probe; Protease

Abbreviations: ABP, activity-based probe; Abz, *o*-aminobenzoic acid; AMC, 7-amino-4-methyl coumarin; APC, Antigen presenting cell; BHQ3, Black hole quencher-3 dye; Cat, cysteine cathepsin; DMF, N,N-Dimethylformamide; Dnp, 2,4-dinitrophenyl; DTT, dithiothreitol; ESI-HRMS, High resolution electrospray ionization mass spectrometry; HEPES, 4-(2-Hydroxyethyl)piperazine-1-ethanesulfonic acid; Fmoc, fluorenylmethyloxycarbonyl; FRET, Fluorescence Resonance Energy Transfer; HNE, human neutrophil elastase; HCTU, 2-(6-Chloro-1-H-benzotriazole-1-yl)-1,1,3,3-tetramethylammonium hexafluorophosphate; KO, knockout; LHVS, morpholinourea-leucinyl-homophenylalanine-vinyl-sulfone; MMP, Matrix metalloproteinase, NIRF, near infrared fluorescence; NMP, 1-methyl-2-pyrrolidone; PR3, proteinase 3; Q-TOF, Quadrupole time-of-flight; RP-HPLC, reversed phase high performance liquid chromatography; RPMI 1640 medium, Roswell Park Memorial Institute 1640 medium; SBP, substrate-based probe; SPPS, solid phase peptide synthesis; TFA, trifluoroacetic acid; WT, wild type.

1. Introduction:

Cysteine cathepsins are papain-like proteases (C1 family, clan CA) [1], which consists of eleven members in humans: cathepsins B, C, F, H, K, L, S, O, V, W, and X [2]. Cysteine cathepsins have long been perceived as housekeeper enzymes, primarily involved in the recycling and degradation of proteins in lysosomes [3]. This view has evolved considerably with the demonstration of their distinctive involvement in specific biological processes (e.g. maturation of thyroid hormones, activation of neutrophil granule-associated proteases, bone resorption, matrix remodeling, pulmonary homeostasis or hair cycle control) and their identification as valuable prognostic biomarkers [2,4–11]. Cathepsins are also deleterious contributors to a wide range of pathophysiological events (e.g. atherosclerosis, adiposity, osteoporosis, arthritis, metastasis, or fibrosis) [12–21]. Cysteine cathepsins primarily localized in endosomal/lysosomal compartments, however they can be secreted and some of them are found extracellularly active (see for review: [22]), favoring pathophysiological processes (e.g. invasiveness of transformed cells at the initial stage of tumor formation) [16,17]. Even though their precise role and individual contributions are still partially misunderstood, cysteine cathepsins have been validated as attractive and accurate targets for novel anti-protease drugs [12,23–26].

Unlike most other family members (including cathepsin L) that display an ubiquitous expression profile, cathepsin S (CatS) expression is essentially restricted to professional antigen-presenting cells (APCs), embracing B cells, dendritic cells (DCs), monocytes and macrophages as well as non-professional APCs such as intestinal epithelial cells [27,28] Although CatS and CatL display similar substrate specificities, CatL favors aromatic residues in the P2 position whereas CatS displays a preference for branched hydrophobic residues [29,30]. Moreover, CatS remains partly active at pH 7.4 while CatL is promptly inactivated at neutral or slightly alkaline pH [26]. CatS contributes to presentation and maturation of major histocompatibility complex class II molecules and DC motility [27,31,32]. An increase in CatS expression has been associated with several illnesses including cancer, atherosclerosis, cystic fibrosis, asthma, emphysema, colitis, irritable bowel syndrome and neuropathic pain [15,26,33,34]. Despite CatS is considered as a clinical biomarker and a relevant therapeutic target, its exact contribution to these diseases remains partly unsolved. The direct assessment of CatS activity within living cells and extracellular milieu using recently developed chemical tools will help to clarify the molecular mechanisms as well dysfunctions that occur during pathophysiological events. The two main strategies of probe design (inhibitor-based *vs* substrate-based probes) to profile protease activity were recently summarized by Turk and

colleagues [35]. See also for examples some outstanding reviews: [36–39]. Both types of probes have been successfully used in a broad range of applications from cell assays to animal models. Briefly, inhibitory activity-based probes (ABPs) react with proteases in stoichiometric ratios. They consist of a reactive functional group (electrophilic warhead) that binds covalently to the active site (via its catalytic nucleophilic residue) of the protease, coupled to a linker or targeting sequence, and a reporter group for visualization. ABPs do not enable signal amplification, which can result in low-intensity signals, but they accurately pinpoint the protease activity. By contrast, substrate-based probes (SBPs) usually contain a peptide (or peptidomimetic) substrate backbone linked to an appropriate tag and a quencher group. Cleavage of SBP by its target can generate strong reporter signal amplification, since a single protease molecule converts several SBPs. However, released reporters may diffuse and could lead to unfocused images.

During the last decade, distinct chemical probes have been developed for assessment of CatS activity, such as a CatS-activatable dendrimer [40,41], peptidyl diazomethyl ketones [37,42], a coumarin-labeled vinyl sulfone tripeptidomimetic [43], "reverse design"-based CatS probes [44–46], NIRF (near infrared fluorescence) non-peptidic quenched ABPs [47,48], and dual-modality (optical and PET/CT) probes [49]. However, given that the extracellular activity of CatS is usually associated with pathophysiological events (e.g. cancer, atherosclerosis or neuropathic pain [26]), a CatS selective probe to assess only secreted active CatS is a highly attractive tool to further understand the complex biology of this protease.

The objective of the present work was to conceive and evaluate a non cell-permeable near infrared fluorescent SBP for monitoring only extracellular CatS activity. We therefore designed a peptide hairpin loop-like structure that consists of a CatS selective substrate sequence and an electrostatic zipper, forcing a close proximity of a N- and C- terminal FRET couple (donor: AlexaFluor680; quencher: BHQ3) [50]. Kinetics constants, signal sensitivity, and physicochemical parameters of the NIRF probe, subsequently referred to as MG101, were determined *in vitro*. Selectivity of MG101 was assessed *ex vivo* by using spleen lysates from CatS knockout (*Ctss*^{-/-}) or wild-type (C57/Bl6 background) mice. Furthermore, the ability of MG101 to specifically detect extracellular CatS activity *in cellulo* was endorsed using human THP-1 macrophages.

2. Material & methods

2.1. Enzymes, substrates and inhibitors

Human cathepsins B, L and H were purchased from Calbiochem (VWR International, Pessac, France). Human CatK was a kind gift from Prof Dieter Brömme (University of British Columbia, Vancouver, Canada). Recombinant human CatS was produced as previously described [51]. Human neutrophil elastase (HNE) and proteinase 3 (PR3) were provided by BioCentrum (Krakow, Poland). Human cathepsin G was from ICN Pharmaceuticals (Costa Mesa, CA, USA). Human aspartic CatD was obtained from Sigma–Aldrich (St Quentin le Fallavier, France). Z-Phe-Arg-AMC and H-Arg-AMC came from Bachem (Bubendorf, Switzerland). Z-Val-Leu-Arg-AMC was supplied by Eurogentec SA (Seraing, Belgium). L-3-carboxy-*trans*-2,3-epoxy-propionyl-leucylamide-(4-guanido)-butane (E-64) was from Sigma-Aldrich. The morpholinourea-leucyl-homophenylalanine-vinyl-sulfone phenyl (Mu-Leu-Hph-VSPh, commonly referred as LHVS) was kindly supplied by Prof James H. McKerrow (Skaggs School of Pharmacy and Pharmaceutical Sciences, University of California, San Diego, CA, USA). The reversible CatS azapeptide inhibitor (i.e compound 1b) was synthesized as described recently [52].

2.2. Peptide chemistry

2.2.1. General information: Unless stated otherwise, all reagents and anhydrous solvents were used without further purification. Protected amino acids, Rink amide ChemMatrix and HCTU were purchased from Merck Biosciences (Nottingham, UK). Peptide synthesis grade DMF was obtained from Applied Biosystems (Courtaboeuf, France). Ultrapure water was prepared using a Milli-Q water system from Millipore (Molsheim, France). Alexa Fluor™ 680 C2 Maleimide was purchased from Thermofisher Scientific (Villebon-sur-Yvette, France). DNP maleimide was purchased from AAT Bioquest (Sunnyvale, CA, USA). BHQ-3 Succinimidyl Ester was purchased from Biosearch technologies (Petaluma, CA, USA). All other chemicals were purchased from Sigma-Aldrich and solvents from SDS-Carlo Erba (Val de Reuil, France) and were used without any further purification. Polypropylene syringes fitted with polypropylene frits were obtained from Torviq (Niles, MI, USA) and were equipped with PTFE (polytetrafluoroethylene) stopcocks (Chromoptic, Courtaboeuf, France).

2.2.2. Peptide characterization and purification: The peptides were analyzed by HPLC and ESI-HRMS mass spectrometry. HPLC analyses were carried out on a LaChrom Elite system consisting of a Hitachi L-2130 pump, a Hitachi L-2455 diode array detector and a Hitachi L-2200 autosampler. The machines were equipped with Nucleosil C18 reversed-

phase columns, 300 Å, 5 µm, 250 × 4.6 mm for analysis (flow rate: 1 mL/min) and 300 Å, 5 µm, 250 × 10 mm for purification (flow rate: 3 mL/min). Solvents A and B were 0.1 % TFA in H₂O and 0.1 % TFA in MeCN, respectively. High resolution ESI-MS analyses (positive mode) were performed on a maXis ultra-high-resolution Q-TOF mass spectrometer (Bruker Daltonics, Bremen, Germany). The observed *m/z* correspond to the monoisotopic ions.

2.2.3. Solid-phase peptide synthesis: Solid-phase peptide synthesis (SPPS) was run on an automated synthesizer 433A from Applied Biosystem using Fmoc/*t*Bu chemistry at a 0.1 mmol scale using Rink amide ChemMatrix[®] as solid support. The 0.1 mmol scale program purchased from the manufacturer was used, with a single coupling followed by capping with acetic anhydride. Briefly, couplings were carried out using a 10-fold excess of protected amino acids, 9.5-fold excess of HCTU and 20-fold excess of *i*Pr₂NEt in NMP (1-methyl-2-pyrrolidone) for 30 min. The protected L-amino acids building blocks used were Fmoc-Ala-OH, Fmoc-Arg(Pbf)-OH, Fmoc-Pro-OH, Fmoc-Glu(*O**t*Bu)-OH, Fmoc-Gly-OH, Fmoc-His(Trt)-OH, Fmoc-Met-OH, Fmoc-Trp(Boc)-OH. The protected D-amino acids building blocks used were Fmoc-D-Ala-OH, Fmoc-D-Arg(Pbf)-OH, Fmoc-D-Glu(*O**t*Bu)-OH. Capping of potential unreacted amine groups was achieved by treatment with acetic anhydride (60 equiv.), *i*Pr₂NEt (15.5 equiv.) and HOBT (1.8 equiv.) in NMP for 7 min. Fmoc deprotection was performed using a 20% piperidine solution in NMP (3 × 3 min). The crude peptide was deprotected and released from the resin with TFA/H₂O/*i*Pr₃SiH/phenol, 87.5/5/2.5/5 for 2 h, and the peptide was precipitated with ice-cold diethyl ether, recovered by centrifugation and washed 3 times with diethyl ether.

2.2.4. Synthesis of MG73: The elongation of the peptide and the introduction of the N-terminal Boc-2-Abz-OH were performed by standard automated solid phase synthesis. Cleavage of the peptide resin using the general procedure gave crude peptide which was used without further purifications. Crude peptide (2 µmol) was dissolved in 400 µL of a 1:1 mixture of DMF and 0.2 M HEPES buffer pH 7.5. The reaction mixture was deoxygenated through several successive vacuum (15 mbar) / argon cycles. Then, a mixture containing DNP-maleimide (2 equiv.) dissolved under argon in 100 µL of deoxygenated DMF was added, the resulting mixture was further deoxygenated and was stirred for 2 h at room temperature. Reaction mixture was analyzed by HPLC to check the total consumption of the peptide. The crude mixture was purified by semi-preparative HPLC (Nucleosil C18 reversed-phase column, 300 Å, 5 µm, 250 × 10 mm; flow rate: 3 mL/min) and lyophilized to yield MG73 peptide as an orange powder (1.1 µmol, 55%). HPLC: semipreparative purification

gradient: 20-45% B/A over 30 min, retention time: 15.6 min. Analytical gradient: 5-65% B/A over 30 min., retention time: 19.5 min. ESI-HRMS (m/z): $[M+H]^+$ calculated for $C_{150}H_{218}N_{54}O_{45}S_2$: 3559.5872, found: 3559.5801.

2.2.5. Synthesis of MG101: The elongation of the peptide was performed by standard automated solid phase synthesis. Cleavage of the peptide resin using the general procedure gave crude peptide which was used without further purifications. Crude peptide (1 μ mol) was dissolved in 400 μ L of a 1:1 mixture of DMF and 0.2 M HEPES buffer pH 7.5. The reaction mixture was deoxygenated through several successive vacuum (15 mbar) / argon cycles. Then, a mixture containing Alexa Fluor™ 680 C2 Maleimide (1 equiv.) dissolved under argon in 100 μ L of deoxygenated DMF was added, the resulting mixture was further deoxygenated and was stirred for 2 h at room temperature. Reaction mixture was analyzed by HPLC to check the total consumption of the peptide. Then, BHQ3-NHS (3 equiv.) was added, the resulting mixture was further deoxygenated and was stirred overnight at room temperature. Reaction mixture was analyzed by HPLC to check the completion of the reaction. The crude mixture was purified by semi-preparative HPLC (Nucleosil C18 reversed-phase column, 300 Å, 5 μ m, 250 \times 10 mm; flow rate: 3 mL/min) and lyophilized to yield MG101 as a deep blue powder (0.43 μ mol, 43%). HPLC: semipreparative purification gradient: 5-65% B/A over 30 min, retention time: 18.5 min. Analytical gradient: 30-50% B/A over 30 min, retention time: 22.4 min. ESI-HRMS (m/z): $[M+H]^+$ calculated for $C_{205}H_{286}BrN_{60}O_{51}S_5$: 4642.9417, found: 4642.9369.

2.3. Physico-chemical characterization of MG101

The stability of MG101 (0.5 μ M) was evaluated by incubation at 37°C in different buffers of increasing pH: 0.1 M glycine-HCl buffer pH 2.2, 0.1 M sodium acetate buffer 0.1 M pH 4.2, 0.1 M sodium acetate buffer pH 5.2, 0.1 M sodium acetate buffer pH 5.5, 0.1 M sodium phosphate buffer pH 7.2, 0.1 M sodium phosphate buffer, pH 7.4, and 0.1 M HEPES buffer pH 8.2 (0-60 min). Then, CatS (5 nM) was added and the fluorescence release (λ_{ex} : 682 nm; λ_{em} : 702 nm) was recorded (Cary eclipse spectrofluorimeter, Agilent Technologies, France). Alternatively, MG101 (0.5 μ M) was incubated in the presence of increasing concentrations of NaCl (0-2 M) at 37°C and the fluorescence release (i.e. corresponding to a lack of self-quenching) was monitored. Further the possible consequence of an intermolecular quenching associated to the release of imaging reporters following the hydrolysis of MG101 was assessed by incubation of CatS (5 nM) with increasing amounts of the probe (0.5, 1, 2, 4, 8, and 16 μ M) at 37°C in 0.1 M sodium acetate buffer pH 5.5, containing 2 mM DTT, 1 mM

EDTA, and 0.01% Brij 35) (λ_{ex} : 682 nm; λ_{em} : 702 nm). The same experiences were repeated for MG73 (λ_{ex} : 320 nm; λ_{em} : 420 nm).

2.4. Enzymatic assays

2.4.1. Selective cleavage of MG101 and MG73: Ethylene diamine tetra acetic acid (EDTA), polyethylene glycol lauryl ether (Brij35), nonyl phenoxy polyethoxy ethanol (NP40), dithiothreitol (DTT) were obtained from Sigma-Aldrich. The activity buffer of cysteine cathepsins was 0.1 M sodium acetate buffer pH 5.5, containing 2 mM DTT, 1 mM EDTA, and 0.01% Brij 35. Alternatively, enzymatic assays were repeated in 0.1 M sodium phosphate buffer, pH 7.4, containing 2 mM DTT, 1 mM EDTA and 0.01% Brij 35. Moreover, activity buffers were 50 mM HEPES buffer, pH 7.4, NP40 0.05%, 150 mM NaCl for neutrophil elastase and proteinase 3, 50 mM HEPES buffer, pH 7.4, NP40 0.05%, 100 mM NaCl for CatG, and 0.1 M sodium citrate buffer, pH 4.0 for aspartic CatD, respectively. Proteases (10 nM) were incubated 5 min at 37°C in their respective activity buffer prior addition of MG101 (1.5 μM). Enzymatic activity was recorded by recording the fluorescence release (λ_{ex} : 682 nm; λ_{em} : 702 nm) (Cary eclipse spectrofluorimeter, Agilent Technologies, Les Ulis, France). The same conditions were applied for MG73 (1.5 μM) (λ_{ex} : 320 nm; λ_{em} : 420 nm).

2.4.2. Determination of the second-order rate constants: CatS and CatL were active site titrated using E-64 [53] (spectromicrofluorimeter SpectraMax Gemini, Molecular Devices, Saint Grégoire, France; λ_{ex} = 350 nm, λ_{em} = 460 nm). Z-Phe-Arg-AMC and Z-Leu-Val-Arg-AMC were used as substrate for CatL and CatS, respectively. Second-order rate constants ($k_{\text{cat}}/K_{\text{m}}$) were further determined under pseudo first-order conditions, i.e. using a substrate concentration far below the K_{m} . CatS and CatL (10 nM) were activated for 5 min at 37 °C in the assay buffer prior kinetic measurements. Briefly, the enzymatic activity of CatS and of CatL was followed by monitoring the hydrolysis of MG101 (0.5 μM) (λ_{ex} : 682 nm; λ_{em} : 702 nm) (Cary eclipse spectrofluorimeter). The half-time of the reaction ($t_{1/2}$) was obtained by plotting $[P] = f(t)$, with $k_{\text{obs}} = \ln 2/t_{1/2}$. The value of $k_{\text{cat}}/K_{\text{m}}$ ($\text{M}^{-1}.\text{s}^{-1}$) was deduced from the equation $k_{\text{cat}}/K_{\text{m}} = k_{\text{obs}}/[E]$ (Enzfitter software, Biosoft, Cambridge, UK). Kinetic data were reported as means \pm S.D (n=3). Alternatively, $k_{\text{cat}}/K_{\text{m}}$ values were determined in 0.1 M sodium phosphate buffer, pH 7.4, containing 2 mM DTT, 1 mM EDTA and 0.01% Brij 35. Identical experiments were performed in triplicate for MG73 (λ_{ex} : 320 nm; λ_{em} : 420 nm).

2.5. Detection threshold of MG101

Increasing amounts of CatS (0-5 nM) were incubated in the presence of MG101 (0.5 μ M) in 0.1M sodium acetate buffer, pH 5.5, containing 2 mM DTT, 1 mM EDTA and 0.01% Brij35 (black 96-well microtiter plates, Nunc, Thermofisher Scientific). After 5 min, fluorescence release was measured using IVIS Caliper Lumina XR imaging system (Caliper LifeSciences, Villepinte, France) (excitation filter: λ_{ex} : 675 nm; emission filter: 690-770 nm; 5 second exposure). Similarly, CatS (5 nM) was incubated in the presence of increasing concentrations of MG101 (0-5 μ M), before recording the fluorescence release ($t = 25$ min) as described above. Control experiments were conducted by pre-incubating for 30 min CatS (5 nM) in the presence of an irreversible CatS inhibitor (LHVS, 1 μ M) or a reversible azapeptide CatS inhibitor (compound 1b, 0.5 μ M), prior addition of MG101 (0.5-2 μ M) and recording of the fluorescence release 10 min latter. Data were presented on color scale overlaid on a grayscale photograph (microplate wells). They were quantified as total radiant efficiency (photons (p) per second (s) per cm^2 per steradian (sr) [photons/s/ cm^2 /sr]) within a circular region of interest (1×10^3 pixels) using the Living Image 4.3.1 software (Caliper Life Sciences).

2.6. Selective hydrolysis of MG101 by CatS

2.6.1. Hydrolysis of MG101 by murine spleen lysates: Mice were housed in accordance with the Animal (Scientific Procedures) Act 1986, following UKCCCR (United Kingdom Co-ordinating Committee on Cancer Research) guidelines and approved by the Ethical Review Committee with Queen's University Belfast. Spleen lysates from CatS knockout (*ctss*^{-/-}) mice or wild-type (C57/Bl6 background) mice were prepared as described elsewhere [52]. After centrifugation (13,000 g for 10 min at 4 °C), the protein concentrations in supernatants were determined with the bicinchoninic acid assay kit (BCA protein assay kit, Interchim, Montluçon, France). MG101 (2 μ M) was added to spleen supernatants (10 μ g protein/assay) and the fluorescence release was monitored (λ_{ex} : 682 nm; λ_{em} : 702 nm) (Cary eclipse spectrofluorimeter). Selectivity of MG101 hydrolysis by wild-type splenic extracts was examined by addition of LHVS (5 μ M). Experiments were performed in triplicate.

2.6.2. Hydrolysis of MG101 by secreted cathepsin S from Human THP-1 macrophages: Human THP-1 monocytic cells (LGC Promochem, Molsheim, France) were plated at 100,000 cells into 96-well plates (microplate IbiTreat, Biovalley, Marne-la-Vallée, France) at 37°C, in 5% CO₂, with Gibco RPMI-1640 (Fisher Scientific, Illkrich, France), containing 1.5 g/L sodium bicarbonate, 4.5 g/L glucose, 10 mM HEPES, 1 mM sodium pyruvate, 0.05 mM 2- β -mercaptoethanol. Culture medium was supplemented by 10% heat-

inactivated fetal bovine serum and 1% penicillin/streptomycin (LGC Standards SARL, Molsheim, France). At day 0, differentiation of monocytes into macrophages was initiated by addition of 162 nM PMA (phorbol 12-myristate 13-acetate, Sigma–Aldrich) then handled as reported elsewhere [54]. At day 6, macrophage-free culture medium (100 μ L) was withdrawn and instantly transferred to black 96-well plates containing 0.1 M sodium phosphate buffer, pH 7.4, 2 mM DTT (final volume: 200 μ L). Culture medium was incubated with MG101 (2 μ M) and the emitted signal was monitored for 0-60 min (IVIS Caliper Lumina XR imaging system (λ_{ex} : 675 nm; λ_{em} detection range: 690-770 nm; 5 s exposure). Analysis of the fluorescence release per well was achieved by using the Living Image 4.3.1 software. Experiments were repeated in the presence of heat-inactivated culture medium (boiling for 5 min) and LHVS (10 μ M), respectively.

2.6.3. Immunochemical analysis: Culture media of THP-1 cells were withdrawn in a preservative buffer (0.1 M sodium acetate buffer, pH 5.5, containing 0.5 mM Pefabloc, 0.5 mM EDTA, 1 mM *S*-methyl thiomethanesulfonate, 0.04 mM pepstatin A) at both day 0 and day 6, then concentrated 10-fold (Vivaspin concentrator tube, exclusion limit 2,000, Sartorius AG, Göttingen, Germany). Protein concentrations were determined by Bradford assay (Bio-Rad, Hercules, CA, USA). Samples were prepared in Laemmli buffer and boiled for 5 min. Concentrated culture media (30 μ g/well) was loaded onto 12% SDS-PAGE, and electrophoresis was carried out under reducing conditions. The separated proteins were transferred to a nitrocellulose membrane (Amersham Biosciences, Buckinghamshire, UK). The membranes were blocked with 5% nonfat powdered milk in PBS, 0.1% Tween 20 (PBS-T). Following incubation (overnight, 4 °C) with a goat anti-human CatS (1:1000; R&D systems, Minneapolis, MN, USA), a rabbit anti-goat IgG-peroxidase conjugate (1:5000, Sigma-Aldrich) was added for 1 h at room temperature. Proteins were visualized by chemiluminescence (ECL Plus Western blotting detection system; Amersham Biosciences). In parallel, the concentration of secreted CatS was determined by sandwich enzyme immunoassay (ELISA DuoSet kit, R&D Systems). Absorbance was measured at 492 nm (VersaMax, Molecular Devices, St Grégoire, France). Measurements were done in triplicate.

2.7. Imaging of secreted cathepsin S by confocal microscopy analysis

Human THP-1 cells were cultured as described above. Six days after stimulation with PMA, MG101 (5 μ M) was added directly in the culture medium of differentiated THP-1 macrophages and imaging performed by confocal fluorescence microscopy (Leica SP8 Confocal Microscope, Leica Microsystems, Nanterre, France) at 0, 5 and 60 min. Data were

acquired using white light laser (wavelength 670 nm) with constant microscope settings (laser power, detector gain, and amplification offset). Control experiments were conducted in the presence of pharmacological CatS inhibitors, i.e. compound 1b (10 μ M) and LHVS (10 μ M), respectively.

3. Results & discussion

3.1. Design and characterization of the intramolecularly quenched fluorescent CatS substrate-based probe MG101

The substrate sequence (i.e. CatS recognition domain) was derived from a substrate previously devised for quantification of CatS activity in APCs [55]. The electrostatic zipper corresponded to a short double strand consisting of complementary charges of a polyanionic (D-Glu)₅ segment and a polycationic (D-Arg)₅ motif) covalently linked to the CatS recognition peptide via a (D-Ala)₂ spacer (see schematic representation: Figure 1). A maleimide functionalized fluorescent dye (AlexaFluor680) was linked to an additional C-terminal Cys via a thioether bond, while the N-terminal dark quencher (BHQ3) was conjugated to the peptidyl backbone via an amide bond. The presence of the (D-Glu)₅/(D-Arg)₅ electrostatic zipper ensures close proximity between the donor group AlexaFluor680 and BHQ3, leading to a potent intramolecular FRET in the absence of proteolytic cleavage. Crucially this zipper has been designed with only five Arg-Glu pairings to ensure the SBP's inability to cross the membrane. It is well established that peptides containing a high proportion of arginines have a unique ability to cross the plasma membrane of cells (cell-penetrating peptides, CPP) [56]. However, homopolymers of fewer than six L- or D-arginines are thought to be ineffective as CPP [57]. Conversely an effective cellular translocation occurs with (L-Arg)₈, the 9-15 mer polyarginines presenting the optimal uptake [58,59].

We analyzed physicochemical properties of the CatS SBP. Spectral properties of MG101 were $\lambda_{\text{excitation}} = 682$ nm, $\lambda_{\text{emission}} = 702$ nm at pH 5.5 (Supplementary file 1a) and $\lambda_{\text{excitation}} = 680$ nm, $\lambda_{\text{emission}} = 703$ nm at pH 7.4 respectively (following dequenching by proteolysis). Time- and pH-dependent stability of the intramolecularly quenched fluorescent (IQF) probe was also examined. After 1 h incubation of MG101 in different pH buffers (pH 2.2 - 8.2), no fluorescence signal corresponding to a self-dequenching was observed, confirming that the intramolecular FRET between AlexaFluor680 and BHQ3 was not affected. Subsequent hydrolysis by CatS led to dequenching and release of fluorescence

regardless of preincubation conditions, supporting that the hairpin loop-like structure conferred an essential molecular stability to uncleaved MG101. This was confirmed by incubation of MG101 in the presence of increasing ionic strengths up to 2 M NaCl where no dequenching was observed (Supplementary file 1b). However, as soon as CatS was added to this high salt solution, fluorescence release was observed, confirming that the cleavage within the substrate sequence induced an immediate dissociation of the salt bridges between the intermolecular (D-Glu)₅ and (D-Arg)₅ strands, promoting the dequenching of the bulky hydrophobic donor/acceptor pair (Supplementary file 1b). Cleavage of increasing amounts of MG101 (up to 16 μM) by CatS led to a linear dose-dependent level of emitted fluorescence ($R^2 = 0.9781$), indicating that intermolecular FRET quenching did not occur.

3.2. Kinetics assays

In the presence of cysteine cathepsins B, H, and K, neutrophil serine proteases (i.e. elastase, cathepsin G, and proteinase 3), and aspartic cathepsin D, no detectable release of fluorescence was observed. As well no cleavage products were detected by RP-HPLC, confirming that MG101 is not susceptible to hydrolysis by these enzymes. On the other hand, a fluorescence release was observed for CatS, and to a lesser extent for Cat L at pH 5.5, but only for CatS at pH 7.4. The cleavage site was located at the Gly-Ala amide bond as already reported [55]. Then the second-order rate constants (k_{cat}/K_m) for the hydrolysis of MG101 by CatL and CatS were determined under pseudo-first order conditions (Table 1). MG101 was highly selective for CatS at a neutral pH mimicking the pH of extracellular media. Unlike most of lysosomal cysteine cathepsins, including CatL, that are optimally active in acidic environments and are rapidly inactivated at neutral pH, CatS remains stable and active at pH 7.4 (for review: [26]), highlighting the tremendous pH-driven selectivity of MG101 for CatS. Interestingly, similar specificity constants were obtained for the hydrolysis of the analogous MG73. MG73 was synthesized with the same primary sequence as MG101 (see Figure 1a), except that the AlexaFluor680/BHQ3 couple was substituted by Abz/Tyr(NO₂). Results demonstrate that k_{cat}/K_m values exclusively relied on the peptidyl CatS recognition pattern, and were not influenced by the chemical structures of the FRET donor/quencher pair. We then assessed the sensitivity (i.e. detection limit) of MG101. In the presence of a constant amount of MG101 (0.5 μM), fluorescence release was measured with subnanomolar concentrations of CatS (25 min incubation, IVIS Caliper Lumina XR imaging system) (Figure 2). Alternatively, in the presence of a constant concentration of CatS (5 nM), we detected a fluorescence signal with submicromolar concentration (0.25 μM) of the substrate-based probe

(5 min incubation). The fluorescence release correlated markedly with CatS enzymatic activity, since there was a full impairment of signal in the presence of LHVS (morpholinourea-leucyl-homophenylalanine-vinyl-sulfone phenyl), a selective irreversible CatS inhibitor or compound 1b, a reversible azaGly-containing peptidomimetic CatS inhibitor [52].

3.3. MG101 is a selective and sensitive substrate-based probe of cathepsin S

First, we validated *ex vivo* the selectivity of MG101 using murine spleens from CatS knockout (*ctss* *-/-*) or wild-type (C57/Bl6 background) mice. Supernatants from spleen lysates, the organ in which the expression of CatS is prominent, were prepared and CatS enzymatic activity was monitored. Hydrolysis of MG101 was observed in WT but not in CatS-deficient samples (Figure 3a). Moreover, the peptidase activity was also abolished in the wild type lysates by the addition of LHVS. Next we tested the probe in macrophages that are a known source of CatS, especially in the tumor microenvironment [60]. Myelomonocytic THP-1 cells reproduce most of macrophage characteristics and thus are widely used as an archetypal cellular model. Conversely to undifferentiated monocytes, differentiated THP-1 cells secrete active cysteine cathepsins (with a maximal activity reached at day 6), as observed with alveolar macrophages and activated smooth muscle cells [61–63]. We noticed a similar upregulation of extracellular CatS at day 6 compared to day 0 for THP-1 cells. Both the mature form of CatS and its proform were revealed by immunoblotting in the supernatants of THP-1 macrophages (Figure 3b). Quantitative analysis by an ELISA assay confirmed that differentiation of THP-1 cells was associated to an over secretion of CatS (mean value: 59.64 ng/ml) for THP-1 macrophages at day 6 (i.e. nM concentration range of mature CatS) vs 3.42 ng/ml (mean value) for undifferentiated monocytes at day 0. In agreement with this finding, Schultz and his colleagues reported the presence of active secreted CatS, since a significant amount of a palmitoylated CatS probe was cleaved by extracellular CatS prior to internalization of the lipidated fragment carrying the fluorophore in THP-1 cells [46]. Here the conditioned medium of THP-1 cells was withdrawn at day 6 and incubated with MG101 (Figure 3b). A specific fluorescence release from cleavage of M101 corresponding to extracellular CatS activity was recorded, which could be fully abrogated by heat inactivation or addition of LHVS. Furthermore, differentiated THP-1 cells that are derived from an acute monocytic leukemia patient secrete MMPs, in particular MMP-2 and MMP-9 [64]. In the presence of EDTA (10 mM) as well 1,10-phenanthroline (2 mM), no change in the fluorescence signal was observed endorsing that MG101 was not hydrolyzed by extracellular

MMPs present in the cell supernatant [65]. These data, taken together with the kinetic evaluations, reveal MG101 to be a highly selective substrate-based probe for CatS.

3.4. Imaging of secreted cathepsin S by confocal microscopy

MG101 (5 μM) was added to culture medium of THP-1 cells and NIR fluorescence release was analyzed by confocal microscopy (0-60 min). A detectable level of NIR fluorescence was observed just 5 minutes after incubation (Figure 4a). The emitted fluorescence was found exclusively in the extracellular medium, but importantly not within living THP-1 cells, as supported by bright-field microscopy, thus validating our probe design strategy. Encouragingly, addition of CatS inhibitors, LHVS or compound 1b, abolished the fluorescence release (Figure 4b).

Our data confirmed that MG101 is highly stable under experimental conditions and that no self-dequenching occurred in the absence of enzyme. Moreover, they supported that MG101 is a potent SBP for CatS imaging, using it application to support the observation that differentiated THP-1 macrophages secrete active CatS. Consistent with its substrate-derived backbone, a limitation for the use of MG101 is that the released reporter group (i.e. the peptidyl moiety bearing AlexaFluor680) led to an unfocused fluorescent signal corresponding to its free diffusion into the extracellular medium. Nevertheless, the precision of the NIRF signal associated to an attractive signal-noise ratio should be noted as demonstrated by the very low fluorescence background of the uncleaved probe, following the selective inhibition of CatS (Figure 4b). The excellent turnover rate constant value of MG101 (pH 7.4; $k_{\text{cat}}/K_{\text{m}}=140,000 \text{ M}^{-1} \cdot \text{s}^{-1}$) thereby makes possible to detect *in situ* subnanomolar to nanomolar concentrations of secreted CatS, as demonstrated here for THP-1 macrophages.

Design of selective probes to allow the discriminatory detection/labelling of active proteases in fresh-frozen tissues [49] and live cell imaging [66] has been a major research focus over the last decade. Crucially, some of these visualization tools have shown potential in preclinical research or are in early clinical trials [14]. Although a benzophenone-bearing photoaffinity-based probe that may allow the detection of active CatL secreted by glioblastoma cells has been reported [67], there is currently no wide collection of probes for the direct visualization of secreted cysteine cathepsin proteases. A diverse range of peptidic and non-peptidic probes has been developed for appraisal of CatS activity [37,40–49,68], but to the best of our knowledge, a selective probe for the targeting of only extracellular CatS has not been reported. Given that an increase of CatS expression and secretion is typically linked

to a diverse range of pathophysiological events [26], we urgently need a such innovative tool for monitoring of secreted active CatS. In conclusion present data support that MG101 is a sensitive and appropriate NIRF substrate-based probe for monitoring secretion of CatS by macrophages and other cell types. In addition to ABPs designed by several colleagues to specifically target and image the intracellular activity of CatS, MG101 may represent a convenient and complementary molecular tool for the detection of active extracellular CatS.

Acknowledgments: LHVS, an irreversible inhibitor of cathepsin S, and human cathepsin K were kind gifts from Prof James H. McKerrow (Skaggs School of Pharmacy and Pharmaceutical Sciences, University of California, San Diego, CA, USA) and from Prof Dieter Brömme (University of British Columbia, Vancouver, Canada), respectively. We acknowledge Dr Guillaume Gabant and the mass spectrometry platform of CBM for the MS analyses.

Funding: This work was supported by la Région Centre-Val de Loire, France (FibroCat project; number 201000049823). We acknowledge the Institut National de la Santé et de la Recherche Médicale (INSERM) for institutional funding. MW held a doctoral fellowship from la Région Centre-Val de Loire. MG received financial support during his post-doctoral internship from la Région Centre-Val de Loire.

Competing interests: The authors declare that they have no competing interests.

References

- [1] N.D. Rawlings, A.J. Barrett, P.D. Thomas, X. Huang, A. Bateman, R.D. Finn, The MEROPS database of proteolytic enzymes, their substrates and inhibitors in 2017 and a comparison with peptidases in the PANTHER database, *Nucleic Acids Res.* 46 (2018) D624–D632. doi:10.1093/nar/gkx1134.
- [2] V. Turk, V. Stoka, O. Vasiljeva, M. Renko, T. Sun, B. Turk, D. Turk, Cysteine cathepsins: from structure, function and regulation to new frontiers, *Biochim. Biophys. Acta.* 1824 (2012) 68–88. doi:10.1016/j.bbapap.2011.10.002.
- [3] F. Lecaille, J. Kaleta, D. Brömme, Human and parasitic papain-like cysteine proteases: their role in physiology and pathology and recent developments in inhibitor design, *Chem. Rev.* 102 (2002) 4459–4488.
- [4] M. Fonović, B. Turk, Cysteine cathepsins and extracellular matrix degradation, *Biochim. Biophys. Acta.* 1840 (2014) 2560–2570. doi:10.1016/j.bbagen.2014.03.017.
- [5] B. Turk, D. Turk, V. Turk, Protease signalling: the cutting edge, *EMBO J.* 31 (2012) 1630–1643. doi:10.1038/emboj.2012.42.
- [6] G. Lalmanach, E. Diot, E. Godat, F. Lecaille, V. Hervé-Grépinet, Cysteine cathepsins and caspases in silicosis, *Biol. Chem.* 387 (2006) 863–870. doi:10.1515/BC.2006.109.
- [7] C. Taggart, M.A. Mall, G. Lalmanach, D. Cataldo, A. Ludwig, S. Janciauskiene, N. Heath, S. Meiners, C.M. Overall, C. Schultz, B. Turk, K.S. Borensztajn, Protean proteases: at the cutting edge of lung diseases, *Eur. Respir. J.* 49 (2017). doi:10.1183/13993003.01200-2015.
- [8] T. Reinheckel, J. Deussing, W. Roth, C. Peters, Towards specific functions of lysosomal cysteine peptidases: phenotypes of mice deficient for cathepsin B or cathepsin L, *Biol. Chem.* 382 (2001) 735–741. doi:10.1515/BC.2001.089.
- [9] B. Friedrichs, C. Tepel, T. Reinheckel, J. Deussing, K. von Figura, V. Herzog, C. Peters, P. Saftig, K. Brix, Thyroid functions of mouse cathepsins B, K, and L, *J. Clin. Invest.* 111 (2003) 1733–1745. doi:10.1172/JCI15990.
- [10] O. Vasiljeva, T. Reinheckel, C. Peters, D. Turk, V. Turk, B. Turk, Emerging roles of cysteine cathepsins in disease and their potential as drug targets, *Curr. Pharm. Des.* 13 (2007) 387–403.
- [11] B. Korkmaz, G.H. Caughey, I. Chapple, F. Gauthier, J. Hirschfeld, D.E. Jenne, R. Kettritz, G. Lalmanach, A.-S. Lamort, C. Lauritzen, M. Łęgowska, A. Lesner, S. Marchand-Adam, S.J. McKaig, C. Moss, J. Pedersen, H. Roberts, A. Schreiber, S. Seren, N.S. Thakker, Therapeutic targeting of cathepsin C: from pathophysiology to treatment, *Pharmacol. Ther.* (2018). doi:10.1016/j.pharmthera.2018.05.011.
- [12] L. Kramer, D. Turk, B. Turk, The Future of Cysteine Cathepsins in Disease Management, *Trends Pharmacol. Sci.* 38 (2017) 873–898. doi:10.1016/j.tips.2017.06.003.
- [13] J.-C. Lafarge, N. Naour, K. Clément, M. Guerre-Millo, Cathepsins and cystatin C in atherosclerosis and obesity, *Biochimie.* 92 (2010) 1580–1586. doi:10.1016/j.biochi.2010.04.011.
- [14] M. Vizovišek, M. Fonović, B. Turk, Cysteine cathepsins in extracellular matrix remodeling: Extracellular matrix degradation and beyond, *Matrix Biol.* (2018). doi:10.1016/j.matbio.2018.01.024.
- [15] G. Lalmanach, A. Saidi, S. Marchand-Adam, F. Lecaille, M. Kasabova, Cysteine cathepsins and cystatins: from ancillary tasks to prominent status in lung diseases, *Biol. Chem.* 396 (2015) 111–130. doi:10.1515/hsz-2014-0210.
- [16] M.M. Mohamed, B.F. Sloane, Cysteine cathepsins: multifunctional enzymes in cancer, *Nat. Rev. Cancer.* 6 (2006) 764–775. doi:10.1038/nrc1949.

- [17] O.C. Olson, J.A. Joyce, Cysteine cathepsin proteases: regulators of cancer progression and therapeutic response, *Nat. Rev. Cancer.* 15 (2015) 712–729. doi:10.1038/nrc4027.
- [18] J. Reiser, B. Adair, T. Reinheckel, Specialized roles for cysteine cathepsins in health and disease, *J. Clin. Invest.* 120 (2010) 3421–3431. doi:10.1172/JCI42918.
- [19] O. Vasiljeva, B. Turk, Dual contrasting roles of cysteine cathepsins in cancer progression: apoptosis versus tumour invasion, *Biochimie.* 90 (2008) 380–386. doi:10.1016/j.biochi.2007.10.004.
- [20] Y. Yasuda, J. Kaleta, D. Brömme, The role of cathepsins in osteoporosis and arthritis: rationale for the design of new therapeutics, *Adv. Drug Deliv. Rev.* 57 (2005) 973–993. doi:10.1016/j.addr.2004.12.013.
- [21] S. Ketterer, A. Gomez-Auli, L.E. Hillebrand, A. Petrera, A. Ketscher, T. Reinheckel, Inherited diseases caused by mutations in cathepsin protease genes, *FEBS J.* 284 (2017) 1437–1454. doi:10.1111/febs.13980.
- [22] K. Brix, A. Dunkhorst, K. Mayer, S. Jordans, Cysteine cathepsins: cellular roadmap to different functions, *Biochimie.* 90 (2008) 194–207. doi:10.1016/j.biochi.2007.07.024.
- [23] M. Drag, G.S. Salvesen, Emerging principles in protease-based drug discovery, *Nat. Rev. Drug Discov.* 9 (2010) 690–701. doi:10.1038/nrd3053.
- [24] F. Lecaille, D. Brömme, G. Lalmanach, Biochemical properties and regulation of cathepsin K activity, *Biochimie.* 90 (2008) 208–226. doi:10.1016/j.biochi.2007.08.011.
- [25] B. Turk, Targeting proteases: successes, failures and future prospects, *Nat. Rev. Drug Discov.* 5 (2006) 785–799. doi:10.1038/nrd2092.
- [26] R.D.A. Wilkinson, R. Williams, C.J. Scott, R.E. Burden, Cathepsin S: therapeutic, diagnostic, and prognostic potential, *Biol. Chem.* 396 (2015) 867–882. doi:10.1515/hsz-2015-0114.
- [27] K. Honey, A.Y. Rudensky, Lysosomal cysteine proteases regulate antigen presentation, *Nat. Rev. Immunol.* 3 (2003) 472–482. doi:10.1038/nri1110.
- [28] E.R. Unanue, V. Turk, J. Neefjes, Variations in MHC Class II Antigen Processing and Presentation in Health and Disease, *Annu. Rev. Immunol.* 34 (2016) 265–297. doi:10.1146/annurev-immunol-041015-055420.
- [29] D. Brömme, P.R. Bonneau, P. Lachance, A.C. Storer, Engineering the S2 subsite specificity of human cathepsin S to a cathepsin L- and cathepsin B-like specificity, *J. Biol. Chem.* 269 (1994) 30238–30242.
- [30] R. Vidmar, M. Vizovišek, D. Turk, B. Turk, M. Fonović, Protease cleavage site fingerprinting by label-free in-gel degradomics reveals pH-dependent specificity switch of legumain, *EMBO J.* 36 (2017) 2455–2465. doi:10.15252/embj.201796750.
- [31] J.A. Villadangos, R.A. Bryant, J. Deussing, C. Driessen, A.M. Lennon-Duménil, R.J. Riese, W. Roth, P. Saftig, G.P. Shi, H.A. Chapman, C. Peters, H.L. Ploegh, Proteases involved in MHC class II antigen presentation, *Immunol. Rev.* 172 (1999) 109–120.
- [32] G. Faure-André, P. Vargas, M.-I. Yuseff, M. Heuzé, J. Diaz, D. Lankar, V. Steri, J. Manry, S. Hugues, F. Vascotto, J. Boulanger, G. Raposo, M.-R. Bono, M. Roseblatt, M. Piel, A.-M. Lennon-Duménil, Regulation of dendritic cell migration by CD74, the MHC class II-associated invariant chain, *Science.* 322 (2008) 1705–1710. doi:10.1126/science.1159894.
- [33] N.N. Jimenez-Vargas, L.A. Pattison, P. Zhao, T. Lieu, R. Latorre, D.D. Jensen, J. Castro, L. Aurelio, G.T. Le, B. Flynn, C.K. Herenbrink, H.R. Yeatman, L. Edgington-Mitchell, C.J.H. Porter, M.L. Halls, M. Canals, N.A. Veldhuis, D.P. Poole, P. McLean, G.A. Hicks, N. Scheff, E. Chen, A. Bhattacharya, B.L. Schmidt, S.M. Brierley, S.J. Vanner, N.W. Bunnett, Protease-activated receptor-2 in endosomes signals persistent pain of irritable bowel syndrome, *Proc. Natl. Acad. Sci. U.S.A.* 115 (2018) E7438–E7447. doi:10.1073/pnas.1721891115.

- [34] P. Zhao, T. Lieu, N. Barlow, M. Metcalf, N.A. Veldhuis, D.D. Jensen, M. Kocan, S. Sostegni, S. Haerteis, V. Baraznenok, I. Henderson, E. Lindström, R. Guerrero-Alba, E.E. Valdez-Morales, W. Liedtke, P. McIntyre, S.J. Vanner, C. Korbmayer, N.W. Bunnett, Cathepsin S causes inflammatory pain via biased agonism of PAR2 and TRPV4, *J. Biol. Chem.* 289 (2014) 27215–27234. doi:10.1074/jbc.M114.599712.
- [35] M. Vizovišek, R. Vidmar, M. Drag, M. Fonović, G.S. Salvesen, B. Turk, Protease Specificity: Towards In Vivo Imaging Applications and Biomarker Discovery, *Trends Biochem. Sci.* 43 (2018) 829–844. doi:10.1016/j.tibs.2018.07.003.
- [36] L.E. Edgington, M. Verdoes, M. Bogyo, Functional imaging of proteases: recent advances in the design and application of substrate-based and activity-based probes, *Curr. Opin. Chem. Biol.* 15 (2011) 798–805. doi:10.1016/j.cbpa.2011.10.012.
- [37] C.S. Hughes, R.E. Burden, B.F. Gilmore, C.J. Scott, Strategies for detection and quantification of cysteine cathepsins-evolution from bench to bedside, *Biochimie.* 122 (2016) 48–61. doi:10.1016/j.biochi.2015.07.029.
- [38] L.E. Sanman, M. Bogyo, Activity-based profiling of proteases, *Annu. Rev. Biochem.* 83 (2014) 249–273. doi:10.1146/annurev-biochem-060713-035352.
- [39] J. Chin, H.-J. Kim, Near-infrared fluorescent probes for peptidases, *Coordination Chemistry Reviews.* 354 (2018) 169–181. doi:10.1016/j.ccr.2017.07.009.
- [40] A.K. Galande, S.A. Hilderbrand, R. Weissleder, C.-H. Tung, Enzyme-targeted fluorescent imaging probes on a multiple antigenic peptide core, *J. Med. Chem.* 49 (2006) 4715–4720. doi:10.1021/jm051001a.
- [41] E. Aikawa, M. Aikawa, P. Libby, J.-L. Figueiredo, G. Rusanescu, Y. Iwamoto, D. Fukuda, R.H. Kohler, G.-P. Shi, F.A. Jaffer, R. Weissleder, Arterial and aortic valve calcification abolished by elastolytic cathepsin S deficiency in chronic renal disease, *Circulation.* 119 (2009) 1785–1794. doi:10.1161/CIRCULATIONAHA.108.827972.
- [42] A. Veilleux, W.C. Black, J.Y. Gauthier, C. Mellon, M.D. Percival, P. Tawa, J.-P. Falgouty, Probing cathepsin S activity in whole blood by the activity-based probe BIL-DMK: cellular distribution in human leukocyte populations and evidence of diurnal modulation, *Anal. Biochem.* 411 (2011) 43–49. doi:10.1016/j.ab.2010.11.022.
- [43] M.D. Mertens, J. Schmitz, M. Horn, N. Furtmann, J. Bajorath, M. Mareš, M. Gütschow, A coumarin-labeled vinyl sulfone as tripeptidomimetic activity-based probe for cysteine cathepsins, *ChemBioChem.* 15 (2014) 955–959. doi:10.1002/cbic.201300806.
- [44] D. Caglič, A. Globisch, M. Kindermann, N.-H. Lim, V. Jeske, H.-P. Juretschke, E. Bartnik, K.U. Weithmann, H. Nagase, B. Turk, K.U. Wendt, Functional in vivo imaging of cysteine cathepsin activity in murine model of inflammation, *Bioorg. Med. Chem.* 19 (2011) 1055–1061. doi:10.1016/j.bmc.2010.10.028.
- [45] D. Caglič, U. Repnik, C. Jedeszko, G. Kosec, C. Miniejew, M. Kindermann, O. Vasiljeva, V. Turk, K.U. Wendt, B.F. Sloane, M.B. Goldring, B. Turk, The proinflammatory cytokines interleukin-1 α and tumor necrosis factor α promote the expression and secretion of proteolytically active cathepsin S from human chondrocytes, *Biol. Chem.* 394 (2013) 307–316. doi:10.1515/hsz-2012-0283.
- [46] H.-Y. Hu, D. Vats, M. Vizovisek, L. Kramer, C. Germanier, K.U. Wendt, M. Rudin, B. Turk, O. Plettenburg, C. Schultz, In Vivo Imaging of Mouse Tumors by a Lipidated Cathepsin S Substrate, *Angewandte Chemie International Edition.* 53 (2014) 7669–7673. doi:10.1002/anie.201310979.
- [47] M. Verdoes, L.E. Edgington, F.A. Scheeren, M. Leyva, G. Blum, K. Weiskopf, M.H. Bachmann, J.A. Ellum, M. Bogyo, A nonpeptidic cathepsin S activity-based probe for noninvasive optical imaging of tumor-associated macrophages, *Chem. Biol.* 19 (2012) 619–628. doi:10.1016/j.chembiol.2012.03.012.

- [48] K. Oresic Bender, L. Ofori, W.A. van der Linden, E.D. Mock, G.K. Datta, S. Chowdhury, H. Li, E. Segal, M. Sanchez Lopez, J.A. Ellman, C.G. Figdor, M. Bogyo, M. Verdoes, Design of a Highly Selective Quenched Activity-Based Probe and Its Application in Dual Color Imaging Studies of Cathepsin S Activity Localization, *J. Am. Chem. Soc.* 137 (2015) 4771–4777. doi:10.1021/jacs.5b00315.
- [49] N.P. Withana, T. Saito, X. Ma, M. Garland, C. Liu, H. Kosuge, M. Amsallem, M. Verdoes, L.O. Ofori, M. Fischbein, M. Arakawa, Z. Cheng, M.V. McConnell, M. Bogyo, Dual-Modality Activity-Based Probes as Molecular Imaging Agents for Vascular Inflammation, *J. Nucl. Med.* 57 (2016) 1583–1590. doi:10.2967/jnumed.115.171553.
- [50] T. Jiang, E.S. Olson, Q.T. Nguyen, M. Roy, P.A. Jennings, R.Y. Tsien, Tumor imaging by means of proteolytic activation of cell-penetrating peptides, *Proc. Natl. Acad. Sci. U.S.A.* 101 (2004) 17867–17872. doi:10.1073/pnas.0408191101.
- [51] J. Sage, F. Mallèvre, F. Barbarin-Costes, S.A. Samsonov, J.-P. Gehrcke, M.T. Pisabarro, E. Perrier, S. Schnebert, A. Roget, T. Livache, C. Nizard, G. Lalmanach, F. Lecaille, Binding of chondroitin 4-sulfate to cathepsin S regulates its enzymatic activity, *Biochemistry.* 52 (2013) 6487–6498. doi:10.1021/bi400925g.
- [52] M. Galibert, M. Wartenberg, F. Lecaille, A. Saidi, S. Mavel, A. Joulin-Giet, B. Korkmaz, D. Brömme, V. Aucagne, A.F. Delmas, G. Lalmanach, Substrate-derived triazolo- and azapeptides as inhibitors of cathepsins K and S, *Eur. J. Med. Chem.* 144 (2018) 201–210. doi:10.1016/j.ejmech.2017.12.012.
- [53] A.J. Barrett, A.A. Kembhavi, M.A. Brown, H. Kirschke, C.G. Knight, M. Tamai, K. Hanada, L-trans-Epoxysuccinyl-leucylamido(4-guanidino)butane (E-64) and its analogues as inhibitors of cysteine proteinases including cathepsins B, H and L, *Biochem. J.* 201 (1982) 189–198.
- [54] T. Garenne, A. Saidi, B.F. Gilmore, E. Niemiec, V. Roy, L.A. Agrofoglio, M. Kasabova, F. Lecaille, G. Lalmanach, Active site labeling of cysteine cathepsins by a straightforward diazomethylketone probe derived from the N-terminus of human cystatin C, *Biochem. Biophys. Res. Commun.* 460 (2015) 250–254. doi:10.1016/j.bbrc.2015.03.020.
- [55] N. Lützner, H. Kalbacher, Quantifying cathepsin S activity in antigen presenting cells using a novel specific substrate, *J. Biol. Chem.* 283 (2008) 36185–36194. doi:10.1074/jbc.M806500200.
- [56] A. Walrant, S. Cardon, F. Burlina, S. Sagan, Membrane Crossing and Membranotropic Activity of Cell-Penetrating Peptides: Dangerous Liaisons?, *Acc. Chem. Res.* 50 (2017) 2968–2975. doi:10.1021/acs.accounts.7b00455.
- [57] D.J. Mitchell, D.T. Kim, L. Steinman, C.G. Fathman, J.B. Rothbard, Polyarginine enters cells more efficiently than other polycationic homopolymers, *J. Pept. Res.* 56 (2000) 318–325.
- [58] S. Futaki, T. Suzuki, W. Ohashi, T. Yagami, S. Tanaka, K. Ueda, Y. Sugiura, Arginine-rich Peptides: an abundant source of membrane-permeable peptides having potential as carriers for intracellular protein delivery, *J. Biol. Chem.* 276 (2001) 5836–5840. doi:10.1074/jbc.M007540200.
- [59] C. Bechara, S. Sagan, Cell-penetrating peptides: 20 years later, where do we stand?, *FEBS Lett.* 587 (2013) 1693–1702. doi:10.1016/j.febslet.2013.04.031.
- [60] V. Gocheva, H.-W. Wang, B.B. Gadea, T. Shree, K.E. Hunter, A.L. Garfall, T. Berman, J.A. Joyce, IL-4 induces cathepsin protease activity in tumor-associated macrophages to promote cancer growth and invasion, *Genes Dev.* 24 (2010) 241–255. doi:10.1101/gad.1874010.

- [61] V.Y. Reddy, Q.Y. Zhang, S.J. Weiss, Pericellular mobilization of the tissue-destructive cysteine proteinases, cathepsins B, L, and S, by human monocyte-derived macrophages, *Proc. Natl. Acad. Sci. U.S.A.* 92 (1995) 3849–3853.
- [62] G.K. Sukhova, G.P. Shi, D.I. Simon, H.A. Chapman, P. Libby, Expression of the elastolytic cathepsins S and K in human atheroma and regulation of their production in smooth muscle cells, *J. Clin. Invest.* 102 (1998) 576–583. doi:10.1172/JCI1181.
- [63] V. Hervé-Grépinet, F. Veillard, E. Godat, N. Heuzé-Vourc'h, F. Lecaille, G. Lalmanach, Extracellular catalase activity protects cysteine cathepsins from inactivation by hydrogen peroxide, *FEBS Lett.* 582 (2008) 1307–1312. doi:10.1016/j.febslet.2008.03.007.
- [64] F. Chellat, A. Grandjean-Laquerriere, R. Le Naour, J. Fernandes, L. Yahia, M. Guenounou, D. Laurent-Maquin, Metalloproteinase and cytokine production by THP-1 macrophages following exposure to chitosan-DNA nanoparticles, *Biomaterials.* 26 (2005) 961–970. doi:10.1016/j.biomaterials.2004.04.006.
- [65] G.S. Salvesen, H. Nagase, Inhibition of proteolytic enzymes, in: J.S. Bond, R.J. Beynon (Eds), *Proteolytic enzymes, a practical approach*, 2nd edition, Oxford University Press, Oxford, UK, 2001, pp.105-130.
- [66] L.E. Edgington-Mitchell, M. Bogyo, M. Verdoes, Live Cell Imaging and Profiling of Cysteine Cathepsin Activity Using a Quenched Activity-Based Probe, *Methods Mol. Biol.* 1491 (2017) 145–159. doi:10.1007/978-1-4939-6439-0_11.
- [67] A. Torkar, S. Bregant, L. Devel, M. Novinec, B. Lenarčič, T. Lah, V. Dive, A novel photoaffinity-based probe for selective detection of cathepsin L active form, *Chembiochem.* 13 (2012) 2616–2621. doi:10.1002/cbic.201200389.
- [68] L. Ben-Aderet, E. Merquiol, D. Fahham, A. Kumar, E. Reich, Y. Ben-Nun, L. Kandel, A. Haze, M. Liebergall, M.K. Kosińska, J. Steinmeyer, B. Turk, G. Blum, M. Dvir-Ginzberg, Detecting cathepsin activity in human osteoarthritis via activity-based probes, *Arthritis Res. Ther.* 17 (2015) 69. doi:10.1186/s13075-015-0586-5.

Figure legends:

Figure 1: Design and structures of fluorescent substrate-based probes.

- (a) Structure of MG73.
- (b) Structure of MG101.
- (c) Schematic representation: general principles of MG101 design and NIRF release mode.

Figure 2: Detection threshold of MG101.

- (a) Increasing amounts of CatS (0-5 nM) were incubated in the presence of MG101 (0.5 μ M) in 0.1 M sodium acetate buffer, pH 5.5, containing 2 mM DTT, 1 mM EDTA and 0.01% Brij35. After 5 min, fluorescence release was measured (excitation filter = 675 nm; emission detection filter = 690-770 nm; 5 s exposure; IVIS Caliper Lumina XR imaging system).
- (b) CatS (5 nM) was incubated in the presence of increasing concentrations of MG101 (0-5 μ M), before recording the fluorescence release (t = 25 min).
- (c) Control experiments were conducted by pre-incubating for 30 min CatS (5 nM) in the presence of LHVS (1 μ M) or compound 1b (0.5 μ M), prior addition of MG101 (0.5-2 μ M) and recording the fluorescence release (t = 10 min).

Figure 3: Selective *ex vivo* hydrolysis of MG101 by cathepsin S.

- (a) Hydrolysis of MG101 by CatS knockout or wild-type murine spleen lysates. MG101 (2 μ M) was added to spleen supernatants (10 μ g protein/assay) from CatS knockout (*ctss* *-/-*) mice (grey line) or wild-type (C57/B16 background) mice (black line) and the fluorescence release was monitored (λ_{ex} : 682 nm; λ_{em} : 702 nm; Cary Eclipse spectrofluorimeter). After 5 min, LHVS (5 μ M) was added. Data are expressed as fluorescence intensity (arbitrary units).
- (b) Hydrolysis of MG101 by THP-1 culture medium. At day 6, culture medium of differentiated THP-1 macrophages was withdrawn, transferred to black 96-well plates, and incubated with MG101 (2 μ M). Fluorescence release was monitored at λ_{ex} : 675 nm and λ_{em} detection range: 690-770 nm (IVIS Caliper Lumina XR imaging system) (0 min, black bar; 60 min, grey bar). Analysis of the emitted signal per well was accomplished by using the Living Image 4.3.1 software. Data are expressed as fluorescence intensity (arbitrary units). Experiments were repeated in the presence of heat-inactivated culture medium (control) and LHVS (10 μ M), respectively. Otherwise, aliquots of conditioned medium of both undifferentiated monocytes (day 0) and differentiated THP-1 macrophages (day 6) were removed and the expression level of secreted CatS was analyzed by immunoblotting.

Figure 4: Probing secreted cathepsin S by confocal microscopy.

- (a) At day 6 after PMA-induced differentiation of THP-1 monocytes, the probe MG101 (5 μ M) was directly added to the culture medium. NIRF release was monitored by confocal fluorescence microscopy (laser 680 nm, red) at 0, 5 and 60 min (left panel), using white light as control (right panel).
 - (b) Alternatively, the selectivity of the NIRF signal was confirmed in the presence of pharmacological CatS inhibitors, i.e. compound 1b (10 μ M) and LHVS (10 μ M), respectively (t = 60 min). White light was used as control (right panel).
- All snapshots were obtained by using objective: 40x and scale bar: 50 μ m.

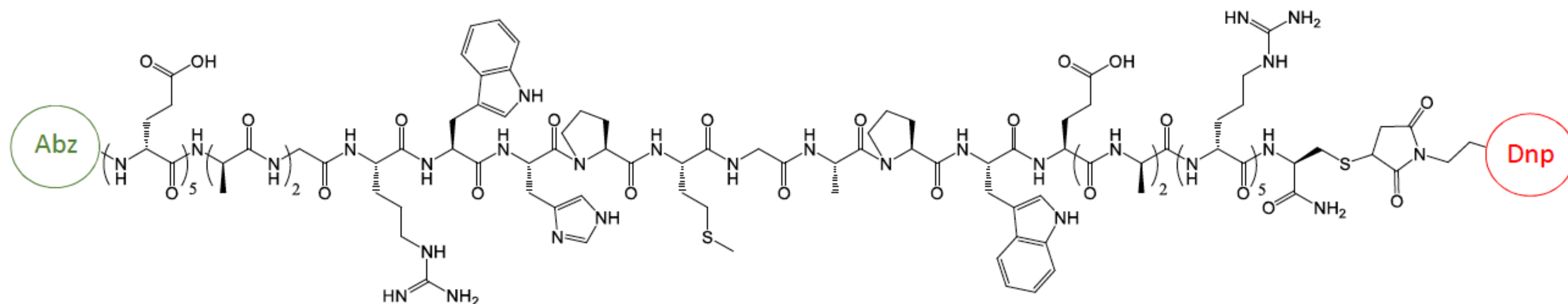
Table I: Kinetic parameters for the hydrolysis of MG73 and MG101.

		k _{cat} /K _m (s ⁻¹ .M ⁻¹)	
		pH 5.5	pH 7.4
MG73	CatS	150,000 ± 8,000	90,000 ± 125
	CatL	15,000 ± 3,000	n.h.
MG101	CatS	300,000 ± 15,000	140,000 ± 70,000
	CatL	10,000 ± 2,000	n.h.
	CatB, H, K	n.h.	n.h.
		k _{cat} /K _m (s ⁻¹ .M ⁻¹)	
MG73, MG101	CatD, CatG, HNE, PR3	n.h.	

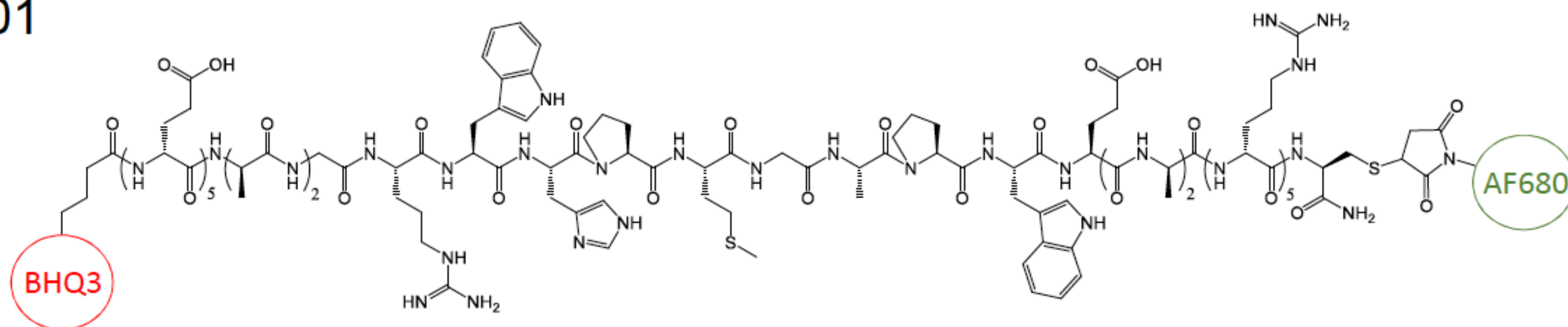
Experiments were carried out as described in the experimental section. Second-order rate constants (k_{cat}/K_m) were determined under pseudo first-order conditions. Values of specificity constants ($M^{-1} \cdot s^{-1}$) were calculated using the Enzfitter software (Biosoft, Cambridge, UK). Kinetic data were reported as means ± S.D (n=3).

n.h., no hydrolysis

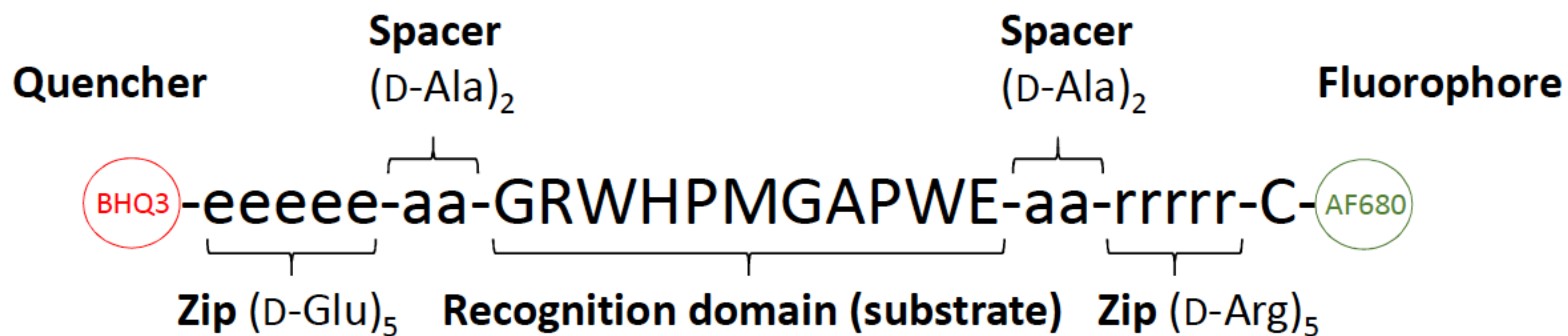
(a) MG73

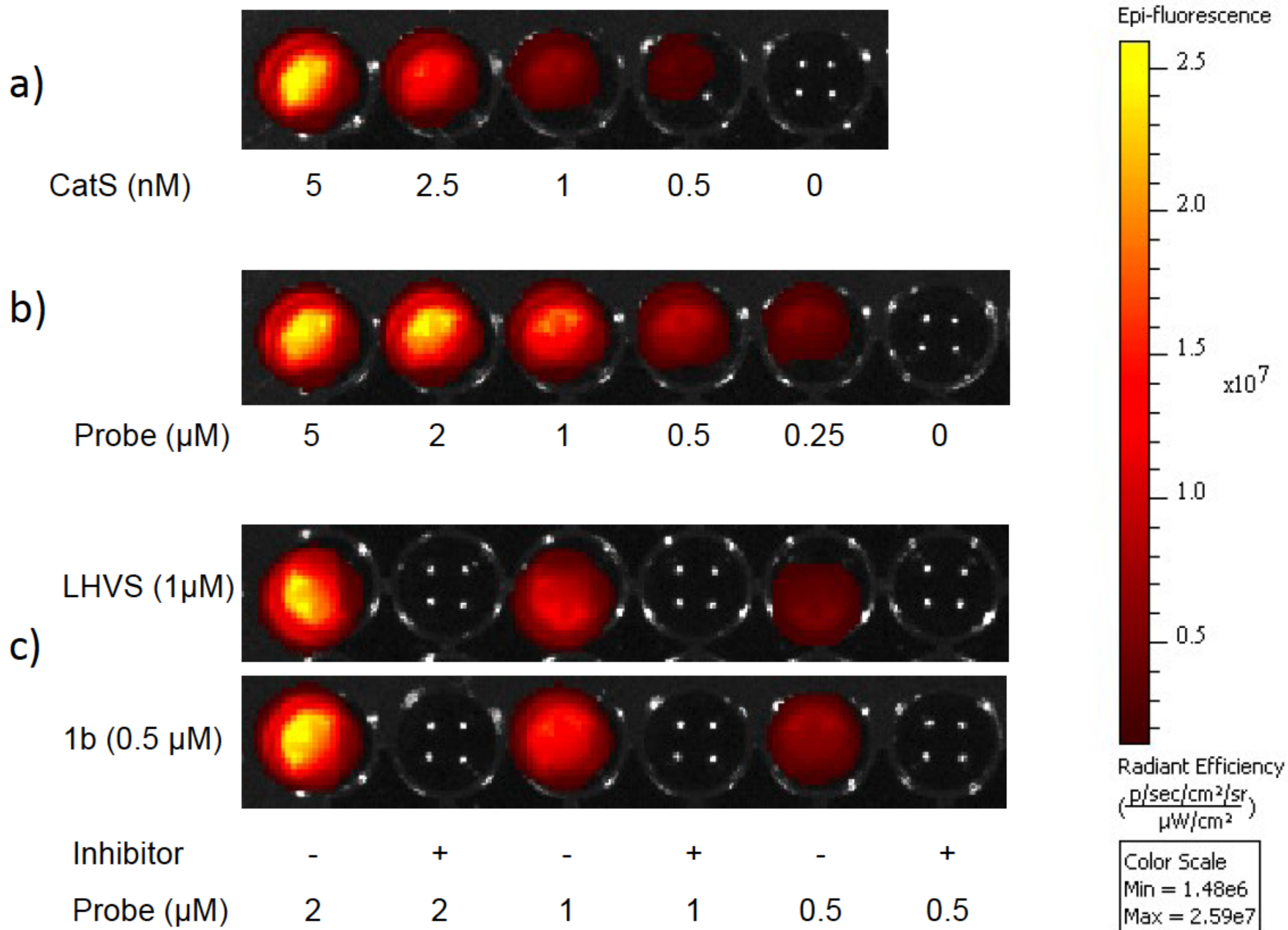


(b) MG101

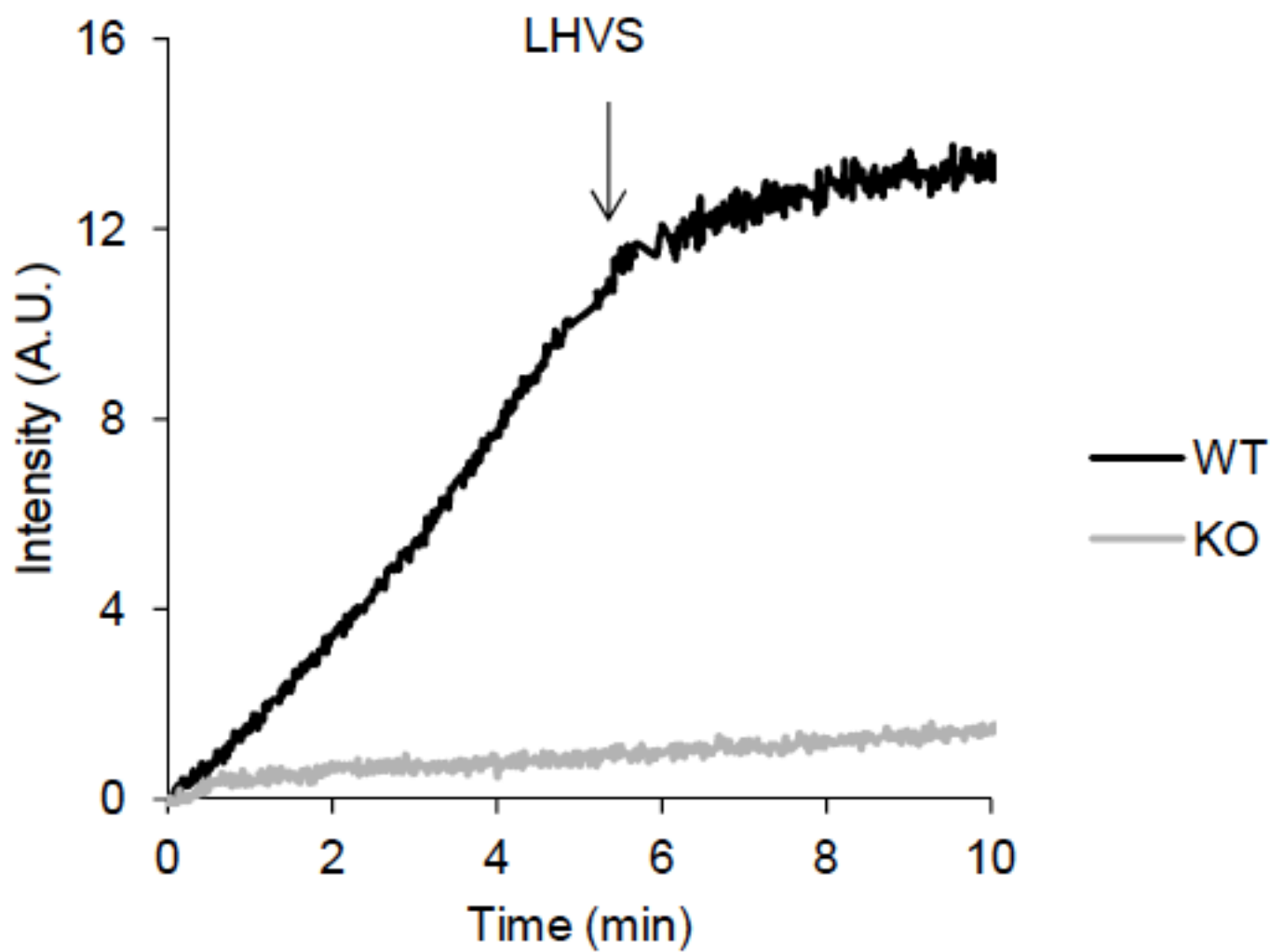


(c) Cartoon representation

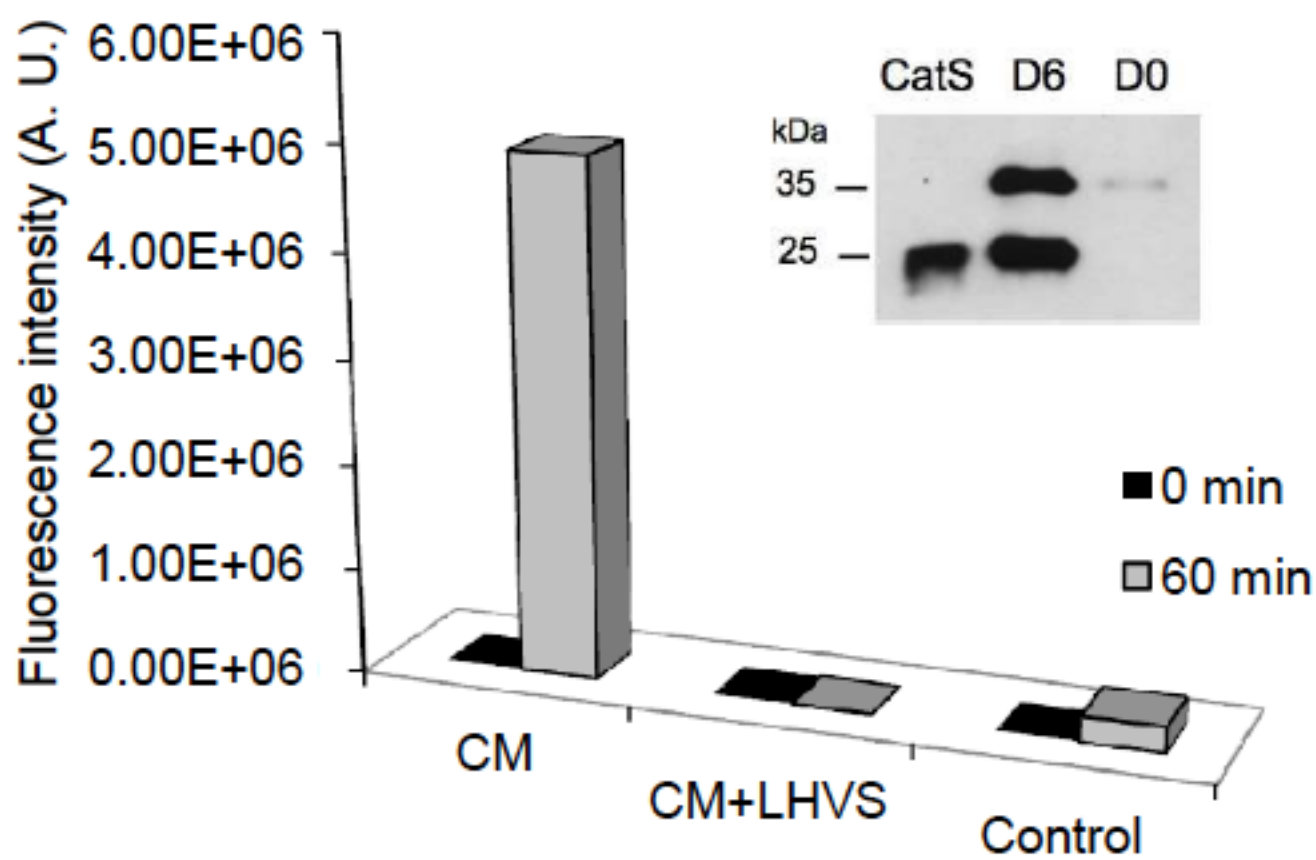




a)

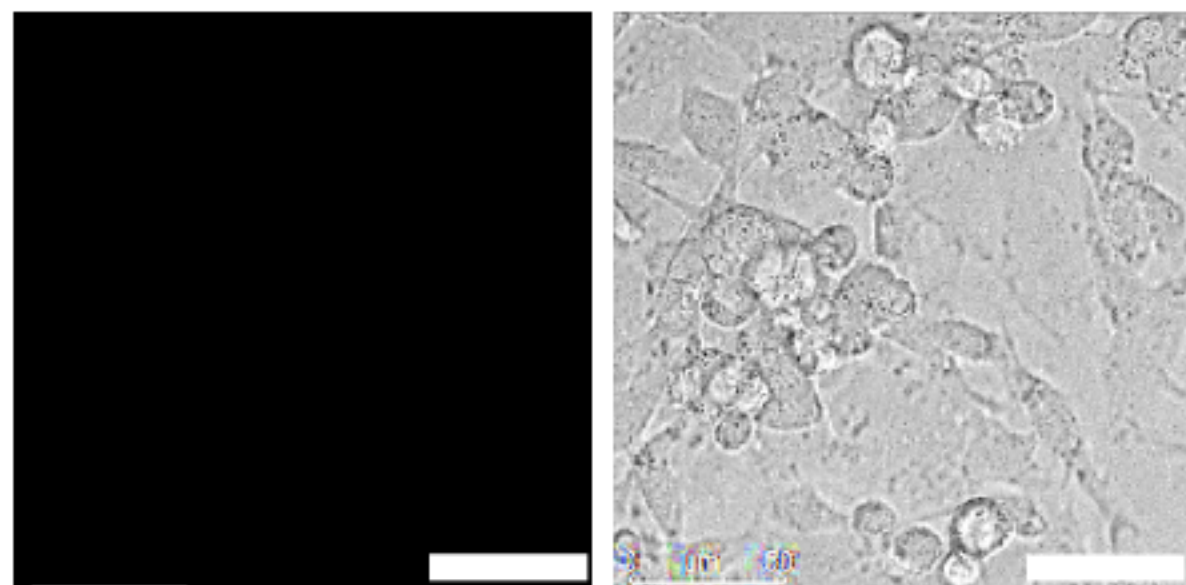


b)

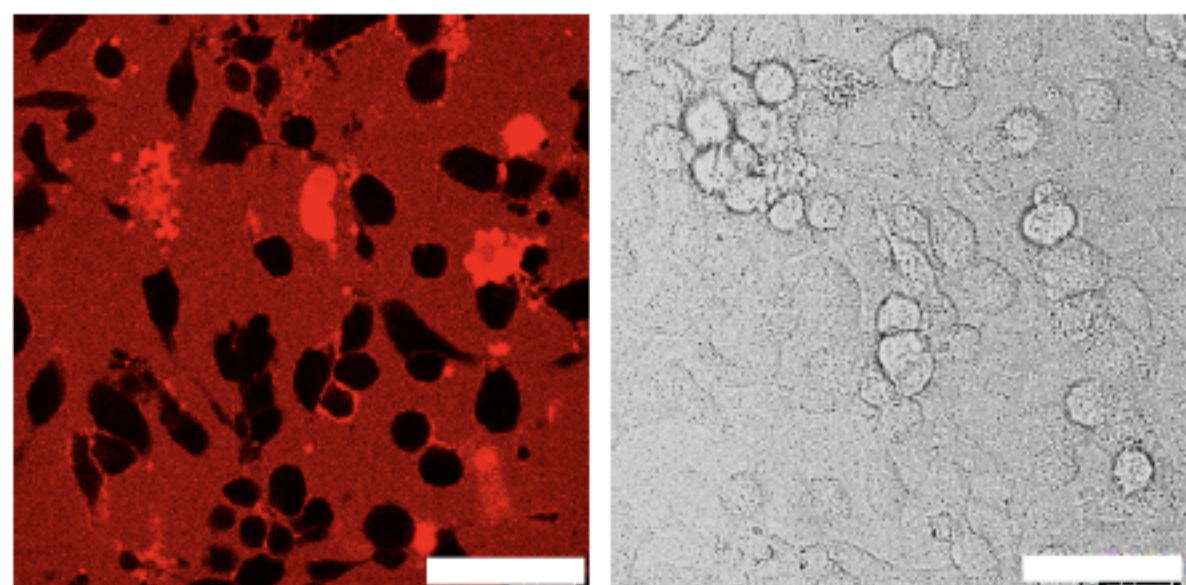


a)

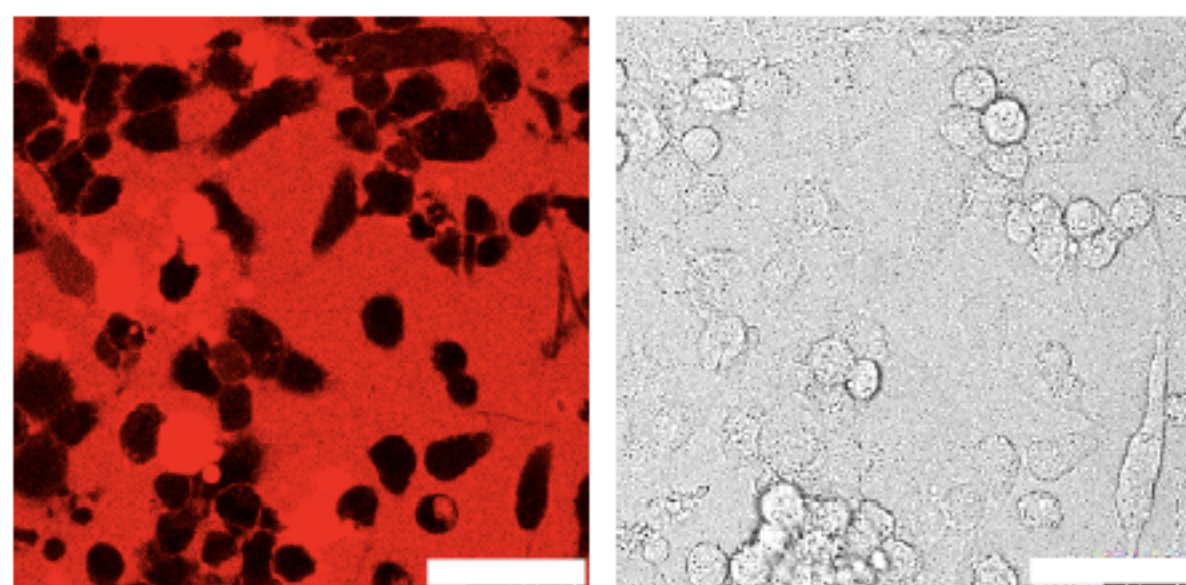
0 min



5 min

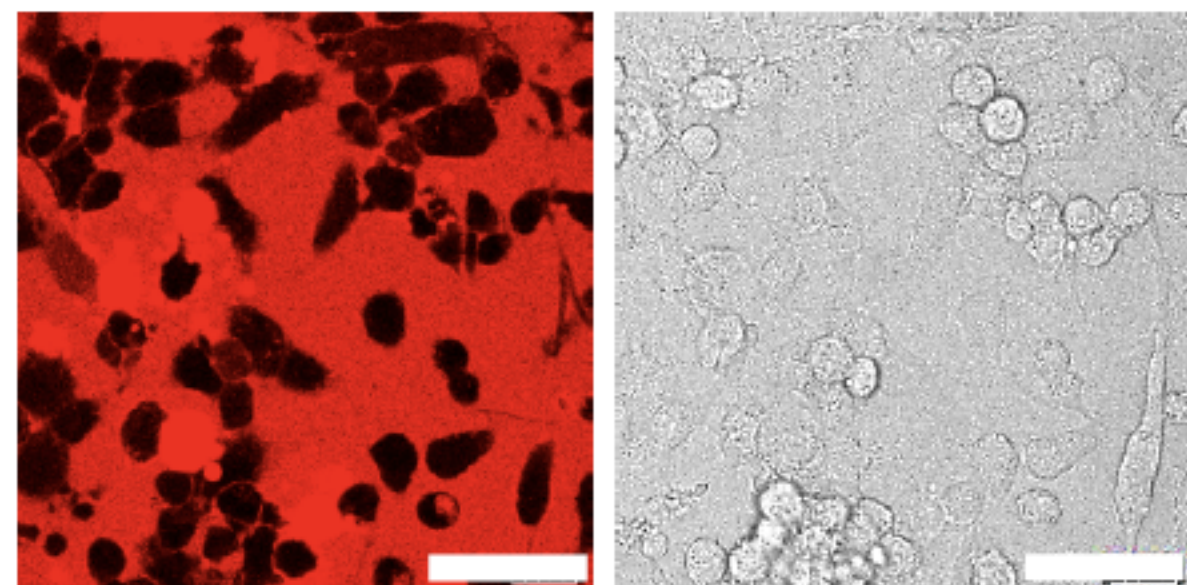


60 min

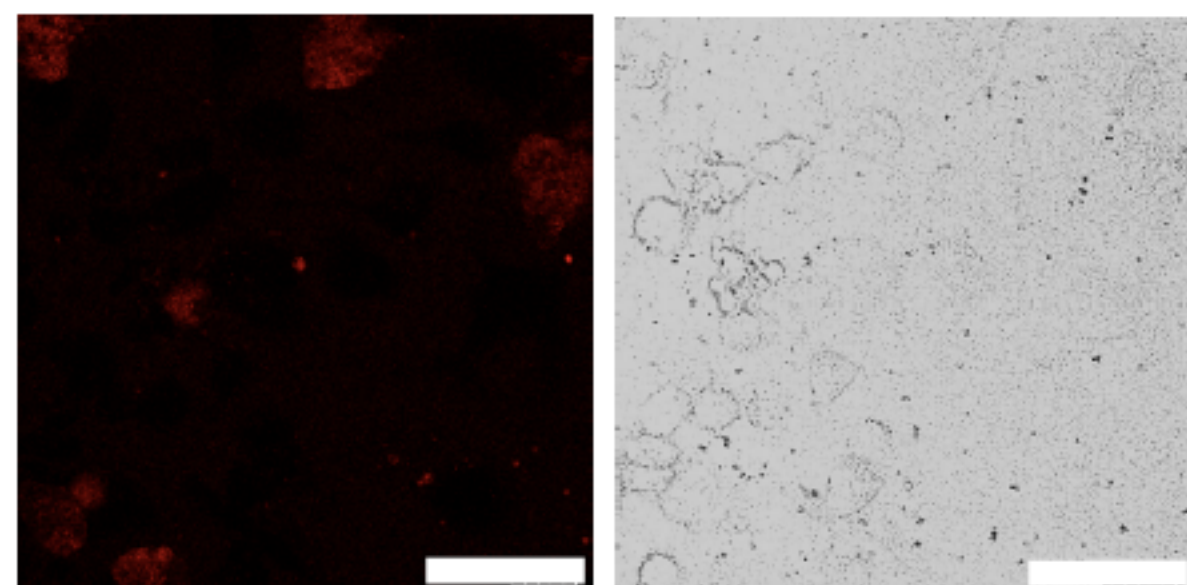


b)

-



+ 1b



+ LHVS

